EPJ Web of Conferences **321**, 03001 (2025) https://doi.org/10.1051/epjconf/202532103001
APITECH-VII-2025

Static and dynamic characteristics of optoelectronic discrete converters for automatic measurement of displacements and dimensions

Umid Kholmatov*, *Sardor* Ulkanov, *Saydolim* Zingirov, *Rustam* Akhunov, *Makhamadyakub* Mansurov, and *Bakhtiyor* Akhmatokhunov

Andijan Machine Building Institute, 170119, Andijan, Uzbekistan

Abstract. This study investigates the static and dynamic characteristics of optoelectronic discrete displacement transducers, with a focus on those utilizing hollow and fiber light guides. These transducers are widely employed in industrial automation due to their simplicity, reliability, cost-effectiveness, and manufacturability. However, certain applications, such as liquid level sensing, object inclination measurement, and automatic piece counting on conveyor lines, remain underdeveloped and understudied. The research examines the reliability of these transducers and their compatibility with microprocessors, highlighting their ability to efficiently convert various physical quantities into discrete outputs by modulating light flux parameters as it propagates from source to receiver. This capability allows for seamless integration with modern monitoring and control systems, presenting significant opportunities for advancement in optoelectronic conversion technology. The study aims to address the growing demand for refined optoelectronic discrete converters that meet contemporary monitoring and control system requirements. By exploring the potential of these transducers in diverse applications, this work contributes to the broader understanding of optoelectronic converters and their role in monitoring and controlling various technological processes. The findings have implications for improving the design and implementation of optoelectronic discrete displacement transducers in industrial settings, potentially leading to more efficient and accurate automation systems.

1 Introduction

The implementation of Uzbekistan's new development strategy for 2022-2026 emphasizes the critical importance of integrating green economy technologies across all sectors. This ambitious plan aims to enhance the economy's energy efficiency by 20% and reduce harmful gas emissions by an equal percentage by 2026. To achieve these goals, technical and technological advancements are considered paramount, particularly in the realm of automated monitoring and control systems.

* Corresponding author: umid.xolmatov.76@mail.ru

In the current landscape of industrial evolution, the significance of converters used to gather information about various technological process parameters is continuously growing. This increase in importance is driven by the need to optimize production processes and develop more sophisticated automated systems. The convergence of automated control systems with information systems is undergoing substantial transformations, propelled by breakthroughs in microelectronics, microprocessor technology, and computer science. Additionally, new processes and phenomena emerging from semiconductor, solid-state, and film technologies, coupled with the application of innovative materials, are contributing to this technological revolution [1].

Optoelectronic converters have emerged as particularly promising tools for measuring displacements and sizes of various objects. Their applications extend to diverse industries, including mining and food processing, where they can be used to measure granules, tubers, grains, seeds, and other materials. Within the realm of optoelectronic converters, those based on hollow fibers represent an under-explored area with significant potential. These converters, when equipped with ring radiation receivers and symmetrically positioned concentrated radiation sources along the hollow fiber's axis, offer the capability to measure small displacements with exceptional sensitivity and accuracy, enabling continuous automatic control [2-3].

The development of such advanced measurement technologies aligns perfectly with Uzbekistan's goals for sustainable development and increased energy efficiency. By improving the precision and efficiency of industrial processes through these innovative converters, industries can reduce waste, optimize resource usage, and ultimately contribute to the nation's environmental targets. Furthermore, the integration of these technologies into automated systems can lead to smarter, more responsive industrial operations that are better equipped to meet the challenges of a rapidly evolving global economy.

As research and development in this field progress, it is crucial to consider not only the technical aspects but also the broader implications for industry standards, workforce training, and economic competitiveness. The successful implementation of these technologies could position Uzbekistan as a leader in sustainable industrial practices, attracting investment and fostering innovation in green technologies.

2 Materials and methods

Optoelectronic converters have emerged as crucial components in modern metrology and measurement systems, offering high precision and reliability in various industrial applications. These devices, particularly those utilizing hollow-core fibers, have gained significant attention due to their unique properties and advantages over traditional solid-core fiber systems. Hollow-core fibers allow for light propagation through air, reducing non-linear effects and enabling enhanced control over light-matter interactions. This technology has found applications in diverse fields, including sensing, imaging, and ultrashort pulse delivery, making it particularly valuable for advanced manufacturing processes that require extreme accuracy and real-time measurements.

An optoelectronic converter based on a hollow fiber (Figure 1) consists of a concentrated radiation source 1, a hollow fiber 2, a radiation receiver 3 and a longitudinal moving reflective disk 4, which modulates the light flux $\Phi_0(x)$ when moving and is rigidly connected to the rod *5*, on which is affected by displacement x_0. The light flux $\Phi_\mathbf{0}$, propagating from the radiation source *1*, located at a distance x_0 from the radiation receiver 3, and passing through the hole, falls on the light-sensitive surface of the disk 4 and further, reflected from it, onto the light-sensitive surface of the radiation receiver 3.

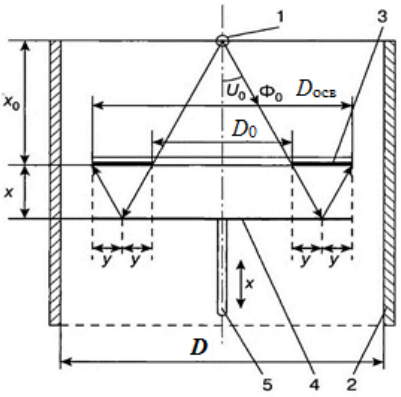

Fig. 1. Physical model of an optoelectronic displacement transducer: *1*-concentrated radiation source; *2*-hollow LED; *3*-radiation receiver; *4*-length reflective disk; *5*-rod.

Figure 2 illustrates the design and measurement setup of an optoelectronic converter used for automated thickness monitoring of tape materials during transport via coils or other mechanisms. The optoelectronic converter is calibrated to a specific nominal thickness, as defined by industry standards and material specifications. As the tape material 12 passes through, the system automatically detects any deviations from this preset thickness. The converter's output signal is then utilized to dynamically adjust and maintain the material's thickness within the required parameters.

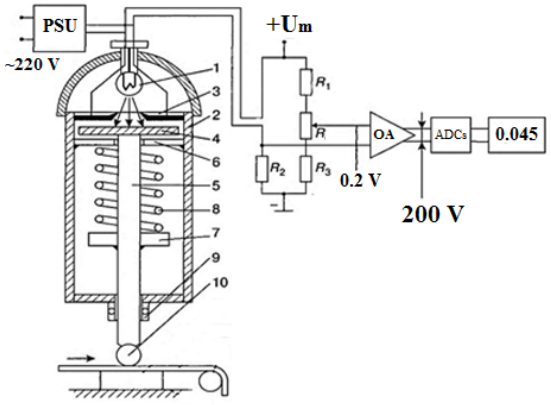

Fig. 2. The optoelectronic displacement transducer: *1*-radiation source (incandescent bulb); *2*-hollow fiber; *3*-ring photoresistor; *4*-reflective disc; *5*-rod; *6* and *7* stops; *8*-spring; *9*-guide tip; *10*-roller.

This automated thickness control system offers real-time monitoring and adjustment capabilities, ensuring consistent quality of the tape material throughout the production process. By continuously measuring and correcting thickness variations, the system helps maintain product uniformity and reduces waste due to out-of-specification materials.

3 Results and discussion

The dynamic characteristic of the ODC corresponds to an aperiodic link of the first order and will significantly manifest itself when the measured value fluctuates (liquid level and during displacements) at high speed.

For example, let the fluctuations in the liquid level occur according to a sinusoidal law:

$$H(t) = H_0 + H * sin\omega t \quad (1)$$

Then the output parameter of the ODC will change according to the law:

$$R_{PR1}(t) = R_{PR1} + \frac{R_{PR1}}{\sqrt{1+(T\omega)^2}} * sin\,(\omega t - f) \quad (2)$$

If the ODC designed to control the liquid level TFL (the time constant of the float or liquid surface) is much greater than the time constant of the radiation receiver T_{RR} $T_{LS} \gg T_{RR}$, then the dynamic characteristic of such TFL will not have a significant impact on the result of level measurement. By analogy with expression (6), at a high pulse repetition rate w, the amplitude of the output signal in accordance with (6) and can be reduced by $1 + T^2\omega^2$ times, and the phase is shifted by an angle $f = arctgT\omega$ when counting a sequence of pulses, taking into account piece products, disk rotation speed and others [4-5].

It is known that the time constant T_{PR} of photoresistors depends on the illumination and on the time they are kept in the dark. With a long exposure of the photoresistors in the dark, the time constant of the rise of the photocurrent T_{frn} increases by 3-4 times. For photodiodes, the time constant is determined by the expression:

$$T_{PR} = R_R * C * (1 + \beta_{Ph} * R_R) \quad (3)$$

where: R_R - load resistance, C - capacitance *p-n* - transition; β_{Ph} is the conversion factor of the feedback link in the block diagram of the photodiode.

The values of the time constants for photoresistors are as follows: $T_{PD} = 0.08 - 0.2\ s$, and for photodiodes $T_{PD} = 10^{-5}s$.

In ODC with transverse movement of the moving element with instantaneous illumination of the entire photoresistor, the increase in the light current $I_c(t)$ occurs according to the expression

$$I_C(t) = I_H + I_{PC} * (1 - e^{-\frac{t_H}{T_H}}), \quad (4)$$

where: I_H I_{PC} are the dark and photocurrent of the photoresistor, respectively; t_H, T_H are, respectively, the rise time of the photocurrent I_{PC}. With instantaneous partial illumination of a completely darkened photoresistor, the current rise is determined from the expression

$$I_{FIH}(t) = \frac{m*U}{R_T\left[K_c(1-m)\left(1-e^{-\frac{t_H}{T_H}}+m\right)\right]+m*R_H}, \quad (5)$$

and the current decay with sequential dimming of the photoresistor

$$I_{FIRP}(t) = \frac{m*U}{R_T\left[K_T(m-1)\left(1-e^{-\frac{t_{RP}}{T_{RP}}}+1\right)\right]+m*R_H}, \quad (6)$$

where: $K_C = \frac{S_C}{S}$ is the ratio of the illuminated part to the entire area of the photoresistor; t_{RP}, T_{RP} are, respectively, the decay time and the decay time constant of the photocurrent; U is the circuit voltage; m is the ratio of the dark resistance to the light resistance of the photoresistor.

Investigation of errors in optoelectronic discrete displacement transducers with hollow and fiber light guides.

The errors of the ODC can be classified according to different criteria:

- according to the degree of uncertainty;
- depending on the conditions of work;
- depending on the source and causes of occurrence, etc.

According to the degree of uncertainty, errors are divided into systematic and random, and depending on the operating conditions - into basic and additional.

It is advisable to estimate the total error of the ODC based on the position of the information theory of measuring devices, from the point of view of which the error of measuring devices is uniquely determined by the value of the entropy error (Δ_e), and the

entropy coefficient K_e depends on the form of the probability density distribution law of element errors.

$$\Delta_e = K_\sigma * \sigma_\Sigma$$

The expression yields the value of the total root-mean-square error σ_Σ for ODC, which has "n" elements.:

$$\sigma_2 = \sqrt{\sigma_1^2 + \sigma_2^2 + \cdots + \sigma_i^2 + \sigma_n^2} \quad (7)$$

$\boldsymbol{\sigma_i}$ - root-mean-square error of the $\boldsymbol{i}$ -th element of the ODC.

Let us determine the calculated value of the ODC error on the basis of the structural diagram. The main elements of the ODC are analyzed below from the point of view of possible sources of errors: photoresistor (PR); bridge measuring circuit (MC); operational amplifier (ADCs) and relay (Re) of the measurement results y k.

The limiting number $\gamma_{PR} = 0.2\%$ normalizes the additive error of PR. A bridge measurement circuit, which has an additive error of $y_{MC} = 0.1\%$, is linked to the PR.

The measuring circuit is powered by a stabilizer (ST), which, together with the amplifier, is powered by a common power supply unit (PSU). An operational amplifier is used as ADCs, which linearizes the static characteristic and has a large input impedance. The output element of the ODC is an electromagnetic relay.

Firstly, we will split up all of the error's components into additive and multiplicative ones. Then, we will find each component's root-mean-square deviation based on the distribution law. Every computation is done using the relative values provided, and one extra inaccurate decimal place is added to the data during intermediate rounding [6-8].

Let the multiplicative error caused by variations in the supply voltage of the MC and ADCs, the additive errors of the PR, MC, and Re, and the temperature dependency of the sensitivity of the amplifier (ADCs) and relay (Re) account for the additive error of the total converter set. The distribution law of the PR error can be interpreted as normal, given an entropy value of $K_{PR} = 2.07$. The standard deviation (RMSD) from this point on is equal to

$$\sigma_{PR} = \frac{\gamma_{PR}}{K_{PR}} = \frac{0.2}{2.07} = 0.097\% \quad (8)$$

Similarly, for the measuring circuit with the normal law of error distribution we have:

$$\sigma_{MC} = \frac{0.2}{2.07} = 0.048\ \% \quad (9)$$

The standard specifies that an allowance for aging is included in the indication of electromagnetic relay inaccuracy. Thus, the value $\gamma_{Re} = 0.8\,\gamma_k$, where γ_{Re} is the main error corresponding to the accuracy class, can be used to determine the maximum error Re.

$\gamma_{\text{Re}} = 0.8 * 0.5 = 0.40\%$. from here on. With an entropy coefficient of $K_{yk} = 1.9$, the law governing the distribution of mistakes in electromechanical devices is nearly trapezoidal. Consequently, we get $\sigma_{\text{Re}} = \frac{\gamma_{\text{Re}}}{1.9} = \frac{0.40}{1.9} = 0.21\%$. The total of the three elements will determine the additive error of the device. As a result, the zero ODC RMS error will be:

$$\sigma_{\text{н}} = \sqrt{\sigma_{PR}^2 + \sigma_{MC}^2 + \sigma_{Re}^2} = \sqrt{0.097^2 + 0.048^2 + 0.21^2} = 0.236\% \quad (10)$$

Figure 3 shows how the entropy coefficients rely on the respective weights of the dispersion must be consulted in order to calculate the entropy coefficient of the total of these errors [8].

$P = \frac{\sigma_{Re}^2}{\sigma_{\text{н}}^2} = \frac{0.21^2}{0.236^2} = 0.79$ is the relative weight of the dispersion of the trapezoidal distribution in the total dispersion. The value of P in this instance is $K_a = 2.0$. The entropy value of the ODC's mistake of zero will thus be as follows:

$$\gamma_{\text{н}} = K_{\text{н}} * \alpha_{\text{н}} = 2.00 * 0.236 = 0.47\% \quad (11)$$

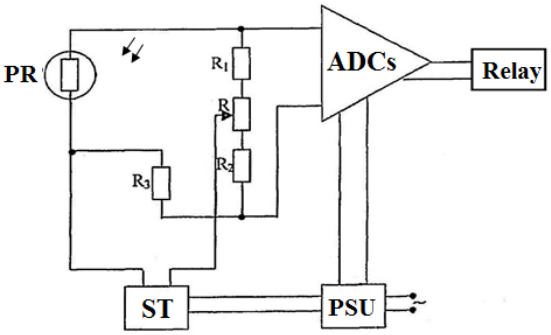

Fig. 3. Measuring circuit of the ODC.

We now take the following beginning data and turn to the summing of multiplicative mistakes. Let $\varphi_{Re} = 0.2\%\ 10^0 K$ be the coefficient of influence of temperature on the sensitivity Re, and let $\varphi_{Re} = 0.1\%\ 10^0 K$ be the amplifier.

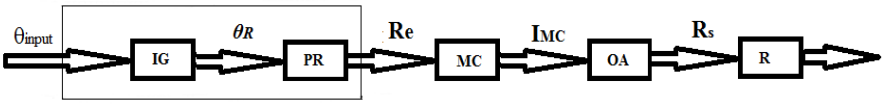

Fig. 4. Structural diagram of the ODC.

Let us assume that the ODC is designed to operate under workshop circumstances at temperatures between +5 and +35 °C, or 20 ± 15 °C, and that all temperatures are equally likely. The multiplicative error's temperature component then has a uniform distribution [2, 4, 5].

$$\gamma_{\theta M} = 0.1 * \frac{15}{10} = 0.15\% \tag{12}$$

and

$$\sigma_\theta = \frac{\gamma_\theta}{K_\theta} = \frac{0.15}{1.73} = 0.087\% \tag{13}$$

Let the voltage variations of the network that powers the considered ODC have a triangle probability distribution law and be within ±10%. A stabilizer with a stabilization factor of $K = 25$ powers the IC. Then, within the bounds $y_{MC} = \frac{10}{25} = 0.40\%$ with RMS, the oscillations in the IC's supply voltage and, subsequently, the multiplicative error of its output voltage, likewise have triangle distributions:

$$\sigma_{ES^1} = \frac{\gamma_{ES}}{\sqrt{6}} = \frac{0.4}{\sqrt{6}} = 0.163\% \tag{14}$$

ODCs is powered by an unstabilized voltage, but due to deep negative feedback, the coefficient of influence of the supply voltage on the gain is reduced to the value $\Psi_{\theta G} = \frac{0.3}{[10(\frac{\Delta U}{U})]}$. As a result, a triangle rule will likewise govern the distribution of the multiplicative error of the ODC, which is brought on by sporadic variations in the supply voltage, inside $y_{ES} = \pm 0.30\%$ with RMS

$$\sigma_{ES^2} = \frac{\gamma_{ES}}{\sqrt{6}} = 0.3\sqrt{6} = 0.122\% \tag{15}$$

Since both voltage fluctuation errors are caused by the same cause, they are correlated with each other and add up algebraically, not geometrically, although each of them is random. That's why:

$$y_S = y_{ES} + \gamma_{\theta M} = 0.3 + 0.4 = 0.7\%$$
$$\sigma_S = \sigma_{ES^2} + \sigma_{ES^1} = 0.122 + 0.163 = 0.285\% \tag{16}$$

Because temperature and voltage fluctuation mistakes are independent of one another, they add up geometrically, that is, with the multiplicative component's RMS.

$$\sigma_{\text{м}} = \sqrt{\sigma_S^2 + \sigma_\theta^2} = \sqrt{0.285^2 + 0.087^2} = 0.298\% \quad (17)$$

The criteria for summing independent mistakes state that the total error of the ODC is equal to the sum of the additive and multiplicative errors:

$$\sigma_\Sigma = \sqrt{\sigma_{\text{н}}^2 + \sigma_{\text{м}}^2} = \sqrt{0.236^2 + 0.298^2} = 0{,}38\% \quad (18)$$

The RMS of the aggregated errors $K_H = 2.00$ and $K_M = 2.04$ are near to each other, and their entropy coefficients are fairly significant.

$$\sigma_{\text{н}} = 0.236 \quad and \quad \sigma_{\text{м}} = 0.298 \quad (19)$$

therefore, we can conclude that the overall entropy coefficient $K_\Sigma = 2.07$

and $$\Delta_{\text{ODC}} = 2.07 * 0.38 = 0.79\% \quad (20)$$

Thus, it is possible to accept the accuracy class of the ODC as not exceeding 1.0%.

Reliability of optoelectronic discrete displacement transducers with hollow and fiber light guides.

Table 1. Types of mechanisms and causes of failure of optoelectronic elements of the ODC.

Types of failures	Failure mechanisms	Reasons for refusals
Degradation of the spectrophotometric parameters of emitters	Degradation of the internal quantum yield, increase in the concentration of nonradiative recombination centers, diffusion of impurities and defects to the transition	Overcurrent, ionizing radiation, defects in the bulk of the semiconductor, mechanical impact on the crystal
	Aging of optical media materials, reduction of light transmittance	Excess temperature, thermal aging of polymers, ionizing radiation
	Deflection of optical media from the crystal, change in light transmittance	Exceeding the temperature gradient, non-compliance of materials according to the CTE
Increasing the dark current of the photodetector	Accumulation of charge on the surface of the photodetector, inversion of the sign of conductivity	The presence of moisture and dirt inside the case, leakage
Breakage of wire connections	Mechanical forces arising from temperature changes, fatigue phenomena	Exceeding the temperature gradient, mismatch of materials according to CTE, low bond strength
	Metallization corrosion	The presence of moisture and dirt inside the case, leakage
	Electromitation	Electric overload
	Breakage due to mechanical influences	Exceeding the limits of resistance to mechanical stress, low strength connections

The reliable operation of the ODC is influenced by the parameters and characteristics of emitters, optical connectors, cable, and photodetector. To obtain optimal matching of the emitter with an optical fiber, it is necessary that the emitter meets a number of requirements. This is, first of all, a small radiating area, commensurate with the diameter of the fiber, which provides a high energy brightness of the source; wavelength of radiation corresponding to the minimum absorption of light when it passes through the fiber; the possibility of simple docking of the emitter with the fiber; preservation of radiating characteristics in a given temperature range and storage of the product under the influence of various mechanical factors [2].

The main parameter when connecting radiation sources with optical fibers is the radiation input coefficient $\eta = \eta_S * \eta_\varphi$, where $\eta_S = \frac{S_F}{S_S}$ is the radiation input coefficient over the area:

$$\eta_\varphi = \frac{\int_0^{\theta Kp} Q_v(\theta) sin\theta d\theta}{\int_0^{\pi/2} Q_v(\theta) sin\theta d\theta} \quad (21)$$

1 - coefficient of input of radiation in angle; S_F is the cross-sectional area of the fiber; S_s - area of the radiating area of the diode: $Q_v(\theta)$ - light energy; θ is the angle.

The radiation power injected into the fiber depends strongly on the numerical aperture of the fiber:

$$\mathrm{P}_{IG} = F_\mathrm{y}\left(\frac{n+1}{2}\right)\frac{S_{FCA}}{S_{ES}}(NA)^2 P_{ES}, \quad (22)$$

where: P_{IG} is the radiation power introduced into the fiber; P_{MCT} is the power emitted by the source; F_y - fill factor; S_{FCA} is the area of the fiber core; S_{ES} is the active area of the source, n is the indicator of the radiation pattern $(cos * \theta)^n$; $NA = n * sin\theta = (n^2 2 - n^2 1)^{\frac{1}{2}}$ - numerical aperture; n_1 is the refractive index of the fiber cladding; n_2 is the refractive index of the fiber core.

NA values are usually in the range of 0.15-0.50. With an increase in NA, the dispersion for LEDs increases, which limits the practically achievable values of the radiation input efficiency when using the maximum possible value of n.

The exponent n for light-emitting diodes is equal to one, and for lasers and LEDs with built-in lenses, the value of n can take values of *2–4*, since injection lasers have narrowed radiation patterns. It is also possible to increase the input coefficient of LED radiation by changing the geometry of the emitter. The emitter output power is concentrated in a beam with angular dimensions of 120°×40° (for diodes with an active edge surface) or corresponds to the Lambertian radiation pattern (for diodes with an active flat surface) [9-10].

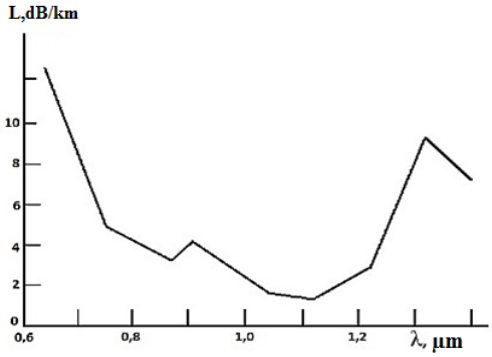

Fig. 5. Signal attenuation curve in glass fiber for various wavelengths.

The losses for the input of radiation into an optical fiber reach a significant value, for example, for an optical fiber with a numerical aperture of 0.14, the losses are about 14 dB for emitters with input of radiation along the p-n junction (edge emitters) and 19 dB for surface emitters. Edge emitters provide higher fiber coupling efficiency than active flat surface diodes, but the lower fiber coupling efficiency is more than offset by their higher radiation power. In general, the reliability of optoelectronic discrete converters with respect to gradual failures, taking into account the operating factors, with an error of not more than 1.0%, is equal to

$$P = \Phi\left(\frac{\Delta S_{max}}{G_s}\right) - \Phi\left(\frac{\Delta S_{max}}{G_s}\right) = \Phi\left(\frac{1}{0.45}\right) - \Phi\left(-\frac{1}{0.45}\right) = 0.97, \quad (23)$$

where: the ratio of the allowable sensitivity ΔS to the maximum sensitivity is

$$\frac{\Delta S}{S_{max}} = 0.45. \quad (24)$$

4 Conclusion

The static characteristics of optoelectronic discrete converters are determined on the basis of a joint consideration of the designs of converters with hollow and fiber light guides and the corresponding measuring circuit with a radiation receiver. It is shown that dividing and bridge measuring circuits are mainly used in optoelectronic discrete displacement transducers.

The static characteristics of relay optoelectronic discrete converters with lumped radiation sources based on hollow and fiber light guides are obtained for longitudinal and transverse displacements of the external modulating body.

The dynamic characteristics of optoelectronic discrete displacement transducers can be described by a first-order aperiodic link, and the curves of the change in the shape of the output signals of discrete transducers significantly depend on the mixing speed of the controlled volume, liquids, piece products and materials.

The reliability of optoelectronic discrete displacement transducers is ensured by the indicator of the sensitivity value in the tolerance field, taking into account the existing factors, and with an allowable error of 1.0%, they will be 0.97%.

The entropy value of the error of discrete optoelectronic displacement transducers is $\Delta_e =$ 0.79 %, which does not exceed the accuracy class of 1.0%.

References

1. U.S. Kholmatov, D.K. Mukimova, E.X. Xalimjonov, A.F. Soliyev, M.M. Maribjonov, M.R. Komilov, M.Shukurov, E3S Web of Conferences **471**, 06015 (2024).
2. P. Castellini, G.M. Revel, E.P. Tomasini, Mechanical Systems and Signal Processing **20(6),** 1265-1285 (2006)
3. G. Berkovic, E. Shafir, Advances in Optics and Photonics **4(4),** 441-471 (2012)
4. S.N. Khonina, N.L. Kazanskiy, M.A. Butt, Biosensors **13**, 835 (2023).
5. T. Bosch, Optical Engineering **40(1),** 20-27 (2001).
6. F.Yıldırım, Sh.Galehdarvand, H.M.Chenari, M.Yılmaz, Ş.Aydoğan, Nanotechnology **35**, 335203 (2024).
7. K.C. Fan, Y. Fei, X. Yu, et al., Measurement Science and Technology **17(3),** 524 (2006).
8. F. Xie, X. Chen, Y. Liu, et al., Optics Express **23(26),** 33947-33963 (2015).
9. J. Friden, *Modern sensors* (Tekhnosphere, 2005).
10. A.L. Gofshtein-Gard, L.M. Kogan, I.T. Rassokhin, Devices and systems **4**, 52-53 (2002).